Controllable bright beam self-focusing initiated by singular dark beams

G. Maleshkov, L. Stojanov, I. Stefanov, A. Dreischuh

Department of Quantum Electronics, Faculty of Physics, Sofia University, Sofia, Bulgaria

ABSTRACT

We study by computer simulations the initial stage of bright background beam self-focusing initiated by the energy density redistribution due to the presence of optical vortex and/or ring dark wave. Local self-focusing Kerr nonlinear medium is considered. When a single ring dark wave is nested on the background, ring radius-to-width ratio Δ=2 promises up to 4 times peak intensity increase at a propagation distance of 2 dark beam diffraction lengths. Δ=6 seems adequate when flat-toped super-Gaussian beam is desired. Self-focusing in bright rings of different radii and even in two coaxial rings (at Δ=3) is observed when initially optical vortex and ring dark wave are simultaneously nested on the background. The detailed numerical analysis of the evolution of azimuthal perturbations confirmed the physical intuition that self-focusing rings of small radii suffer much less (when at all) from ring filamentation, because the spatial frequency of the perturbations on the inner rings appear higher than the critical one.

Keyword list: Kerr nonlinearity, self-focusing, optical vortex, ring dark wave, phase dislocation, modulation stability

1. INTRODUCTION

Propagation of optical beams in nonlinear media (NLM) has been a subject of continuing interest for more than four decades, partially due to the possibility for creation of reconfigurable waveguides through the intensity-dependent refractive index change.[1,2] Particular interest in singular dark beams (optical vortices, one-dimensional dark beams and ring dark waves) is motivated by their ability to propagate as dark spatial solitons or dark solitary waves and to induce gradient optical waveguides in bulk self-defocusing NLM.[1,3,4] Necessary (but not sufficient) condition for this is to propagate them in a self-defocusing NLM, in which the dark beam diffraction is compensated for by the medium's nonlinearity. In contrast to the evolution in self-defocusing NLM, the positive Kerr nonlinearity leads to (accelerated) dark beam broadening and energy density redistribution on the host background beam. As a result, controllable self-focusing of the bright structures on the background could be initiated.[5-7] Many intriguing perturbative nonlinear processes (e.g. cascaded four-wave mixing assisting the white light generation) and non-perturbative processes (e.g. high harmonic generation) take place in transparent nonlinear media of positive nonlinearities. The presented results may appear especially important in such experiments involving dark singular beams (optical vortices, ring dark waves etc.) where accelerated dark beam spreading is accompanied by self-focusing of certain portions of the perturbed host beams.

2. NUMERICAL PROCEDURE

The numerical simulations of the beam propagation along the local Kerr NLM are carried out using the (2+1)-dimensional nonlinear Schrödinger equation (NLSE)

$$i\frac{\partial E}{\partial\left(z/L_{Diff}\right)}+\frac{1}{2}\Delta_T E+n_2\,|\,E\,|^2\,E=0\ ,\qquad (1)$$

which accounts for the evolution of the slowly-varying optical beam envelope amplitude under the combined action of nonlinearity and diffraction. Here Δ_T is the transverse part of the Laplace operator whereas $L_{Diff}=ka^2$ stands for the diffraction length of an 1D *tanh*-shaped dark beam and $sign(n_2)=+1$ means self-focusing nonlinearity. ($sign(n_2)=-1$ and $L_{Diff}=L_{NL}$ are necessary conditions for 1D dark spatial soliton formation). In the above notations, *k* is the wave number inside the medium. The transverse spatial coordinates (*x* and *y*) are normalized to the 1D dark beam width *a*. The model

NLSE we solved by means of the split-step Fourier method with a computational window spanning over 1024x1024 grid points. As a standard test we modeled the formation of a fundamental one-dimensional tanh-shaped dark spatial soliton (Fig. 1, open circles and solid curve). All further numerical simulations are carried out at this background beam intensity. Since the presence of an optical vortex and/or ring dark wave alter (decrease) the initial peak intensity of the background in dependence of the dark structure width a and ring radius Δ, we will further express all propagation distances in units of diffraction lengths $L_{Diff} = ka^2$. The (green) dashed curve in Fig. 1 shows the profile of the input 1D *tanh*-shaped beam after linear propagation over z=6L_{Diff} As seen, the beam broadening is accompanied by noticeable oscillations on the background, which should have, as we will see later, a non-negligible impact on the beam propagation under self-focusing conditions. Similar local intensity increase is seen also when an optical vortex is nested on the background (Fig. 1, inset).

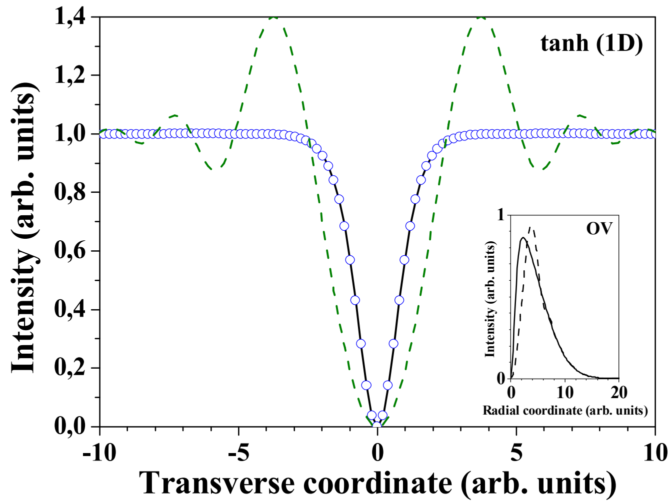

Fig. 1 Calibration calculations for negative nonlinearity: Cross-section of an input one-dimensional (1D) *tanh*-shaped odd dark bam (blue open circles) and of the fundamental 1D dark spatial soliton at z/L_{Diff}=6 (solid curve). Green dashed curve – 1D dark beam diffraction at the same distance. **Inset:** Radial cross-section of an optical vortex at z=0 (solid curve) and after free-space propagation up to z/L_{Diff}=6 (dashed curve), where L_{Diff}, as in the previous case, refers to the diffraction length of the 1D *tanh*-shaped dark beam.

The electric field amplitude of the Gaussian background beam $B(x,y)$ carrying an optical vortex of unit topological charge and/or ring dark wave is assumed to be of the form

$$E(x,y,z=0) = \sqrt{I_0}\,B(x,y)\tanh\left[r(x,y)/a\right]\exp\left[i\varphi(x,y)\right]\tanh\left[(r-\Delta)/a\right]\exp\left[i\Phi(r)\right] \quad , \tag{2}$$

where r and φ are the radial and azimuthal polar coordinates corresponding to Cartesian coordinates x and y, respectively, Δ is the radius of the dark ring, a is the characteristic dark structure width, and $\Phi(r)$ is the dark ring phase distribution

$$\Phi(r) = \begin{cases} -\pi/2 & \text{for } |r| \le \Delta \\ +\pi/2 & \text{for } \ r > \Delta \end{cases} \quad . \tag{3}$$

3. RESULTS AND DISCUSSION

We carefully inspected our data during the calculations and restricted the propagation distances to lengths, at which the peak intensity remained less than 6 times higher than the initial one. This was done in order to keep the slowly-varying envelope approximation valid. Since the most results will be described at z/L_{Diff}=2 and 5, it is worth mentioning, that the pure Gaussian background beam, under perfect conditions (no hot spot formation) and at the already specified intensity, increases its intensity by 4% and 38% for z/L_{Diff}=2 and 5, respectively.

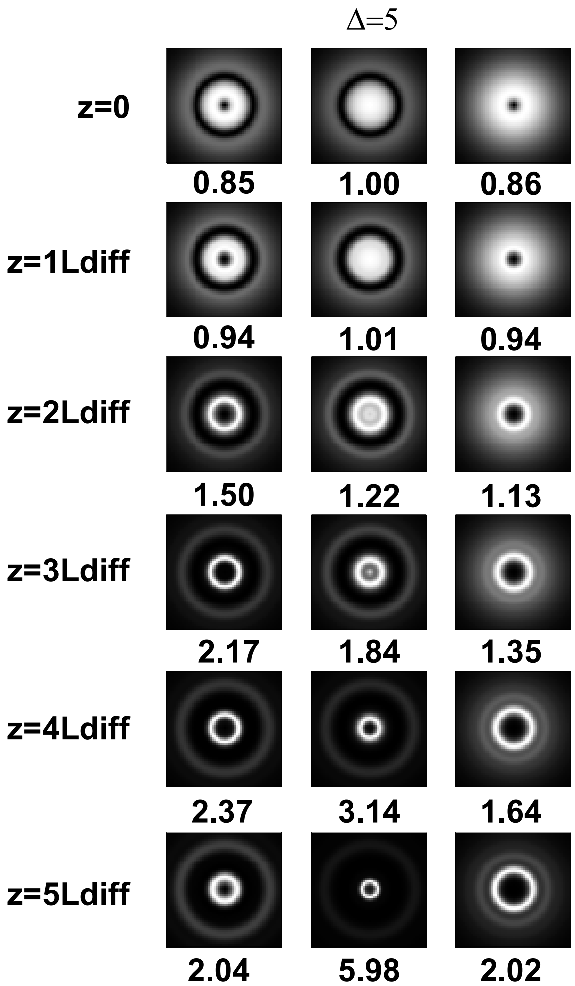

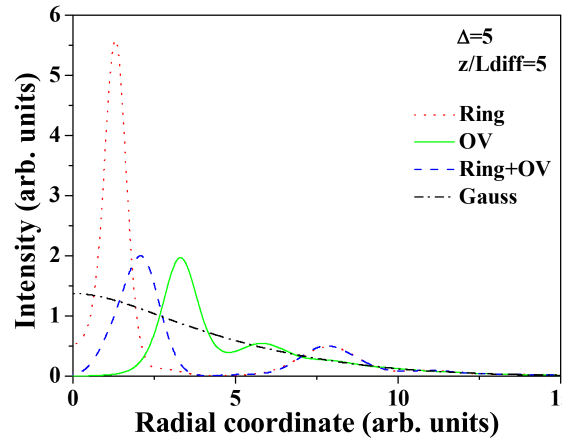

Fig. 3 (above). Radial cross-sections of the background beams with the respective dark structures nested on them after nonlinear propagation distance $z/L_{diff}=5$.

Fig. 2 (to the left) Beam evolution along the nonlinear medium for both OV and ring present (left column), for ring dark wave only (middle column), and for OV centered on the background beam only (right column). The calculations refer to Δ=5. Numbers below each frame – background beam peak intensity at the respective propagation distance.

In Fig. 2 we show the beam evolution along the nonlinear medium for both OV and ring present (left column), for ring dark wave only (middle column), and for OV centered on the background beam only (right column). The initial dark ring radius is always assumed to be Δ=5. The grayscale for each frame is separately normalized, so the most-strongly self-focused bright structure appears on the darkest background. As clearly seen (see also Fig 3, the (red) dotted curve) single dark ring with Δ=5 can force the background to be strongly self-focused (peak intensity increase ~6) under conditions, under which the background beam alone increases its intensity by some 40%. OVs with and without outer dark ring are able to increase twice the bright beam intensity within rings of different radii (see last row of frames in Fig. 2) and the respective radial cross-sections in Fig. 2).

An additional and quite intriguing insight in to the beam reshaping and self-focusing initiation can be gained when following the background beam evolution along the NLM with initial dark rings of different radii nested (see Fig. 4).

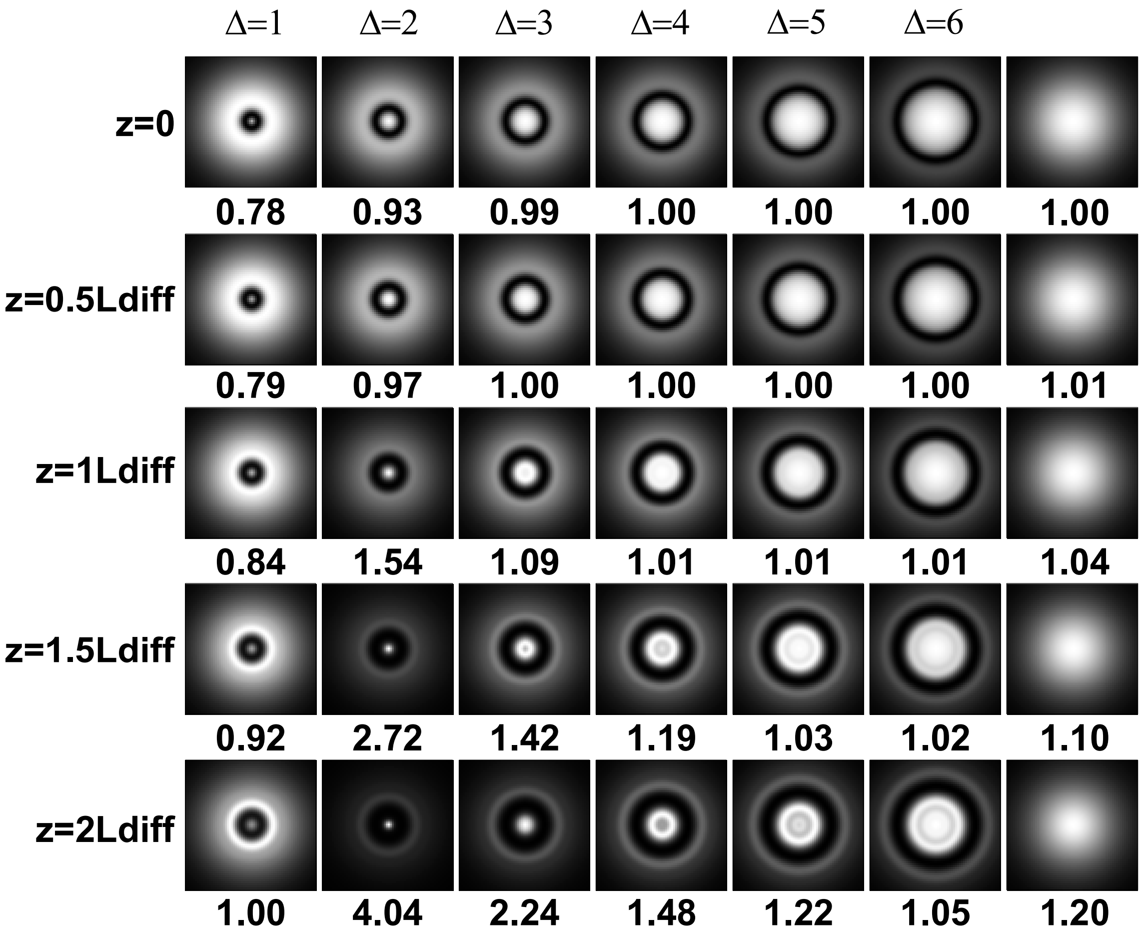

Fig. 4 Beam reshaping and initial stages of self-focusing for background beam propagation along the NLM with initial dark rings of different radii only. Numbers below each frame – background beam peak intensity at the respective propagation distance. Last column – nonlinear evolution of the pure Gaussian background beam.

Note, that in this set of simulations the fastest longitudinal dynamics is observed for Δ=2. That is why the data for Δ=5 only partially cover these shown in the middle column in Fig 2. In this case (Δ=5) the beam reshaping into super-Gaussian like beam at z/L_{Diff}=2 continues and the beam further reshapes in a small ring (z/L_{Diff}=5, see Fig. 2). For Δ=1 the most intense parts of the beam are initially located outside the ring and further the self-focusing ring of relatively large radius should be expected to dominate. For Δ=2 and 3, however, the intense areas of the beam are near its axis and self-focusing in a single filament should be expected (see the second and third left columns in Fig. 4), but with quite different intensity growth speeds. In Fig. 5 we show radial cross-sections of selected cases from these simulations demonstrating that, at a particular nonlinear propagation distance, different beam profiles could be obtained. Note (see also Fig. 6) that in all cases the peak intensities exceed this of a pure Gaussian beam at the same distance. The data shown in Fig. 6 indicate that the bright host beam self-focusing initiated by the ring dark beam has its maximum near dark ring radius Δ=2.

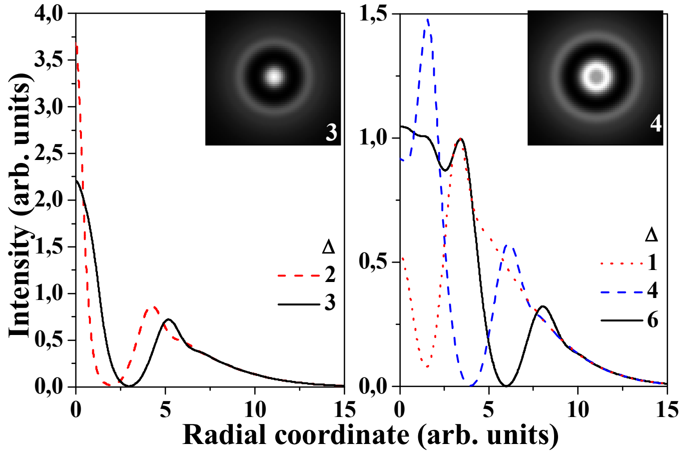

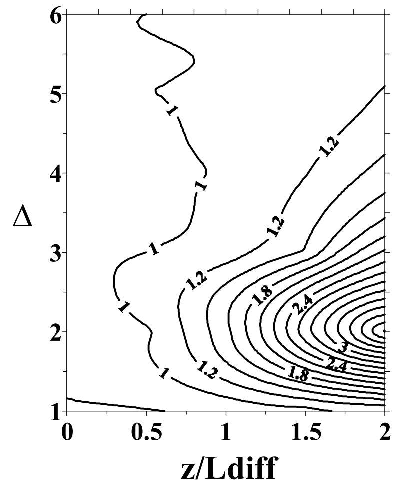

Fig. 5 Radial cross-sections of the background beams carrying only dark rings, after nonlinear propagation distance z/L_{Diff}=2 (see also Fig. 4).

Fig. 6 Peak intensity vs. dark ring radius Δ and propagation distance z/L_{Diff}, corresponding to the results shown in Fig. 4.

We further studied the beam reshaping and self-focusing along the NLM caused by the presence of both singly-charged on-axis vortex and outer ring dark wave of varying radius Δ. Due to the presence of two dark waves on the background, its initial peak intensity becomes reduced and we followed the beam evolution up to z/L_{Diff}=5 (see Fig. 7). For Δ=1 and 2 the initial area of highest beam amplitude/intensity is located outside the ring. Therefore, the background beam self-focusing takes place in rings of large radii (see the left two columns in Fig. 7). For Δ=3, however, simultaneous beam self-focusing in two coaxial rings dominates up to z/L_{Diff}=5. Since the energy reservoir in this case is gradually smaller as compared to the cases Δ=1 and 2, at this distance the peak intensity increases gradually less. Further, for Δ=4…6, the region of initial high field amplitude/intensity is located between the vortex and the ring. Therefore, self-focusing in a single ring structure dominates, but with bright ring radii smaller that these in the cases Δ=1 and 2. In this range (Δ=4…6) the higher the ring radius Δ, the higher the beam peak intensity at z/L_{Diff}=2…5. Since optical vortices are routinely generated with high efficiency by means of spiral phase plates with segments of discrete thicknesses, thy will cause azimuthal perturbations. The influence of these perturbations on the stability of the ring self-focusing will be studied in the last part of this paper.

In Fig. 8 we show radial cross-sections of the background beams carrying optical vortices and dark rings, after nonlinear propagation distance z/L_{Diff}=5, which corresponds to the results shown in Fig. 7. It is naturally to expect and to observe, that the intensity in the vortex core vanishes due to the point phase dislocation. It is interestingly to note that the radial velocity of the dark ring remains relatively small, the phase jump along the ring does not decrease its dislocation amplitude and the intensity vanishes also along the ring arc. In Fig. 9 we show topographical plot of the peak intensity vs. dark ring radius Δ and propagation distance z/L_{Diff}, corresponding to the results shown in Fig. 7. The data indicate that the bright host beam self-focusing initiated by the ring dark beam and the vortex has at least two local maxima near dark ring radius Δ=2 and Δ=6.

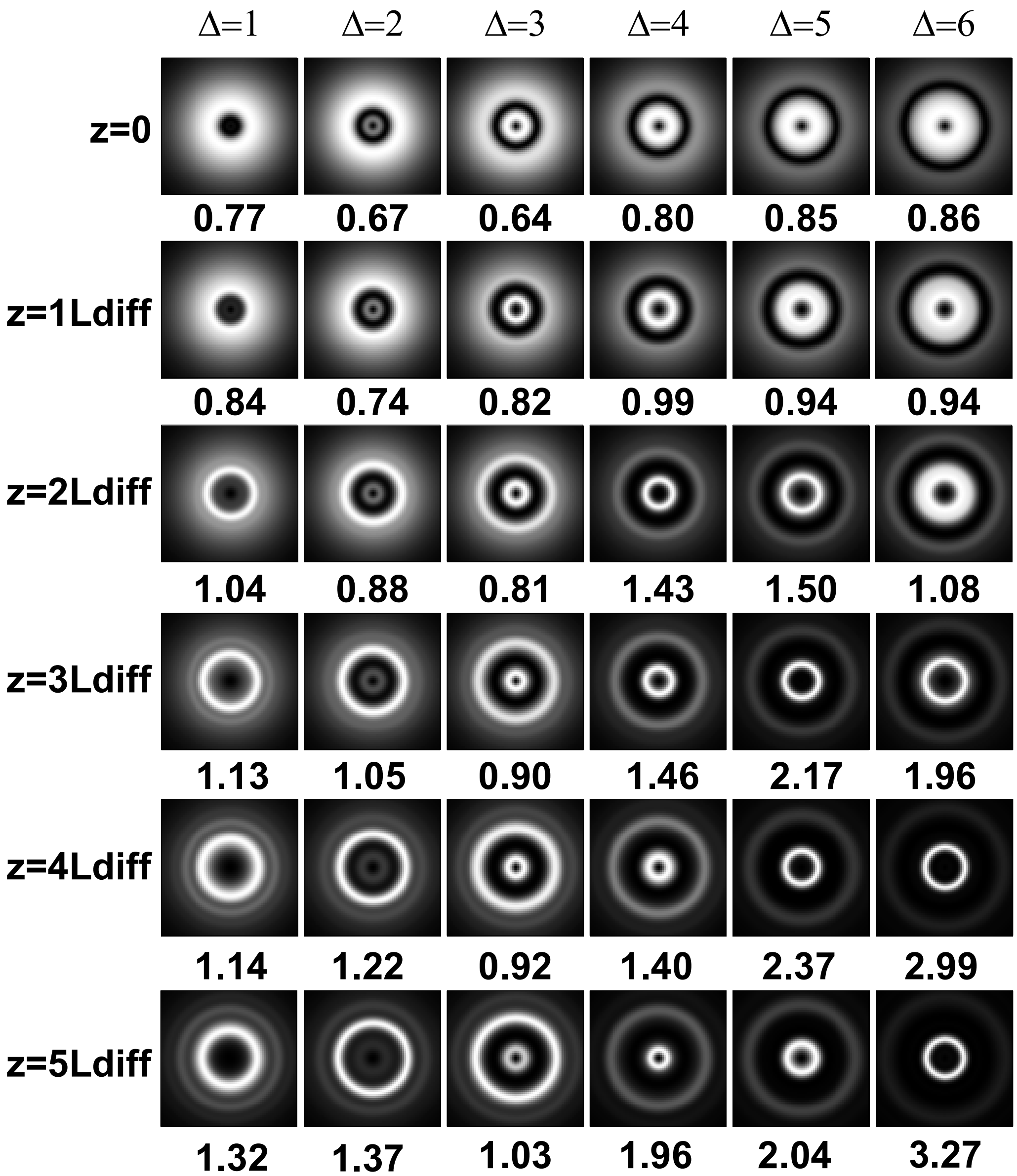

Fig 7. Beam reshaping and self-focusing along the NLM caused by the presence of both singly-charged on-axis vortex and outer ring dark wave of varying radius Δ.

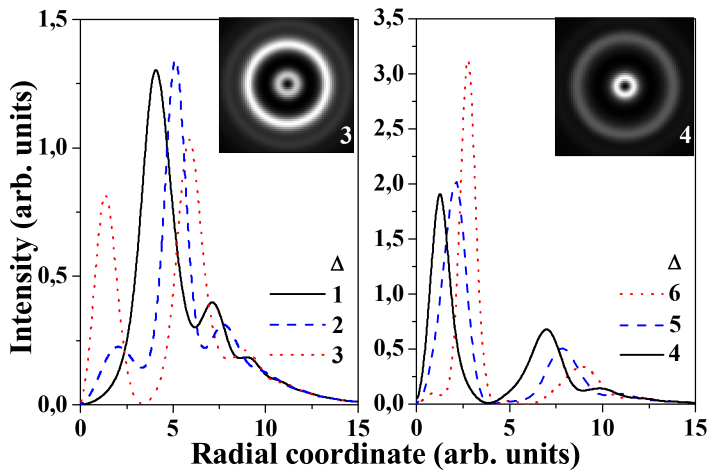

Fig. 8 Radial cross-sections of the background beams carrying optical vortices and dark rings, after nonlinear propagation distance z/L_{Diff}=5 (see also Fig. 7).

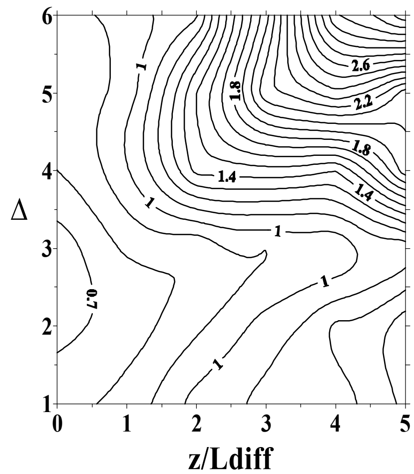

Fig. 9 Peak intensity vs. dark ring radius Δ and propagation distance z/L_{Diff}, corresponding to the results in Fig. 7.

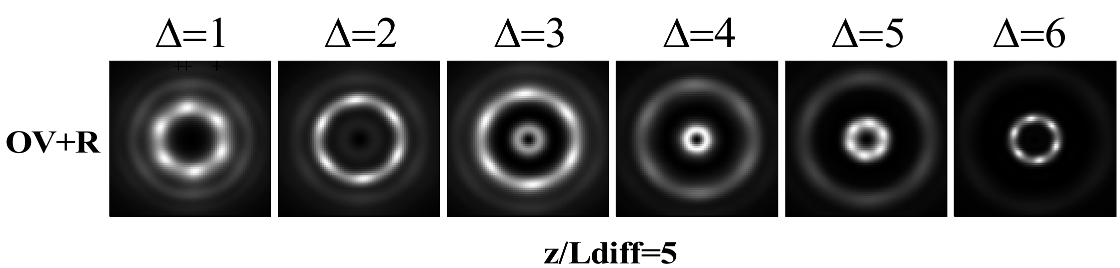

Fig. 10 Evolution of the bright background beam in the presence of both singly-charged on-axis vortex and outer ring dark wave of varying radius Δ for azimuthal perturbation with 6 spatial periods.

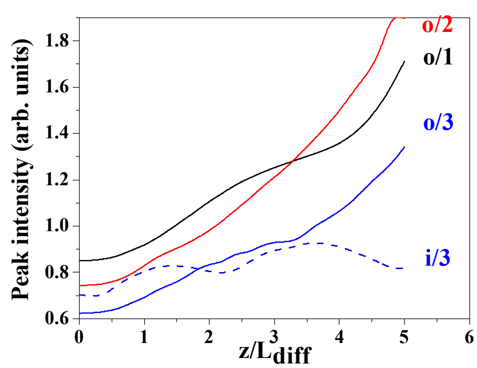

Fig. 11 Peak intensity vs. propagation distance for cases denoted as j/Δ, where j=o means outer ring and j=i means inner ring. Δ is the initial dark ring radius.

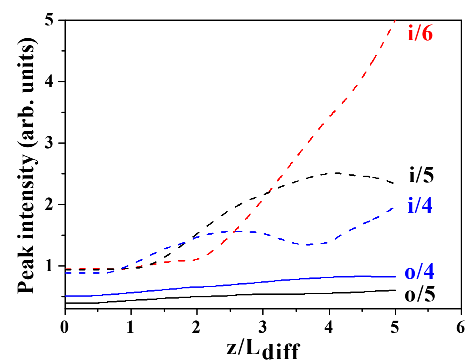

Fig. 12 The same as in Fig. 11, but for different initial dark beam radii.

4. CONCLUSION

The presence and evolution of ring dark beam and/or on-axis optical vortex nested on a bright background beam is noticeably perturbing the host background beam and, in a self-focusing Kerr nonlinear medium, can initiate filamentation of the background beam. Geometry-controlled condition here is the dark ring radius and the presence/absence of an optical vortex. In this way one can relatively easily control the self-focusing longitudinal speed and the self-focusing structure (single peak or bright ring of variable radius). In view of the stability analysis we performed, one can conclude that smaller self-focusing rings should appear more stable against azimuthal perturbations as compared to rings of larger diameters. The presented results may appear especially important in experiments involving cascaded nonlinear frequency mixing of singular beams, in which accelerated dark beam spreading is accompanied by self-focusing of certain portions of the perturbed host beam.

5. ACKNOWLEDGEMENTS

This work was supported by the Science Fund of the Sofia University and, by the NSF-Bulgaria (grants DO-02-0114/2008 and DRNF-02-8/2009).

6. REFERENCES

[1] Stegeman, G. I. and Segev, M., “Optical spatial solitons and their interactions: Universality and diversity,” Science **286**, 1518-1523 (1999).
[2] Kivshar, Yu. S. and Luther-Davies, B., ‘‘Dark optical solitons: physics and applications,” Phys. Rep. **298**, 81-197 (1998).
[3] Swartzlander, Jr., G. and Law, C., ‘‘Optical vortex solitons observed in Kerr nonlinear medium,’’ Phys. Rev. Lett. **69**, 2503–2506 (1992).
[4] Law, C. T., Zhang, X. and Swartzlander, Jr., G. A., ‘‘Waveguiding properties of optical vortex solitons,’’ Opt. Lett. **25**, 55–57 (2000).
[5] Hansinger, P., Dreischuh, A. and Paulus, G. G., "Optical vortices in self-focusing Kerr nonlinear media," Opt. Commun. **282**, 3349-3355 (2009).
[6] Hansinger, P., Dreischuh, A. and Paulus, G. G., "Vortices in ultrashort laser pulses," Appl. Physics B, **104**, 561-567 (2011).
[7] Maleshkov, G., Hansinger, P., Dreischuh, A., Paulus, G. G., “Fractional vortex dipoles of edge-screw type in self-focusing Kerr nonlinear media,” Proc of SPIE **7747,** art. # 77471P (2011).